Prediction of Marine Winds in the New York Bight

JAMES E. OVERLAND[1] AND WILLIAM H. GEMMILL

National Meteorological Center, National Weather Service, NOAA, Washington, D. C. 20233

(Manuscript received 9 March 1977, in revised form 13 May 1977)

ABSTRACT

Comparison is made between wind velocity measurements at two NOAA buoys, EB34 and EB41, located in the New York Bight, and winds extrapolated from nearby coastal stations and inferred from sea level pressure analysis at the National Meteorological Center. The comparison covers 0000 and 1200 GMT observations for November 1975 through March 1976. Surface winds are obtained from gradient winds by means of the analytic single-point boundary layer model proposed by Cardone (1969) and simple empirical relations.

Buoy wind speeds in excess of 10 m s^{-1} accounted for 28% of the observations. For these strong winds, pressure-gradient based estimates provided adequate specifications of surface winds for 81% of the cases, defined by vector error <5 m s^{-1}, and were in general superior to estimates extrapolated from single coastal stations.

Rapid changes in wind speed and direction recorded in hourly buoy data indicate that resolution of winter storms requires pressure analyses on at least a 6 h cycle. The presence of moving storm systems also suggests that the use of coastal station reports can be improved by extrapolation in time as well as space.

1. Introduction

Within the next decade, the understanding of continental shelf circulation will be such that surface current models can be formulated to aid in trajectory forecasting. As with wave forecasts in the open ocean, drift estimates on the continental shelf will strongly depend upon the adequacy of the wind field analysis and forecast. Beardsley and Butman (1974) report that currents in winter on the shelf south of New England are highly correlated with major storms, with current speeds associated with a storm event nearly an order of magnitude greater than the average for the season.

There are three basic approaches for providing winds: 1) extrapolation of wind reports from observing sites; 2) estimation from synoptic pressure and ancillary fields; and 3) the use of a storm model which specifies a detailed wind distribution in terms of gross storm parameters—storm size, intensity and track. We assess the first and second options by systematically comparing wind measurements at two NOAA buoys in the New York Bight with wind estimates derived from sea level pressure analyses and extrapolated from coastal station observations. The data period is November 1975–March 1976. On the basis of one winter's data, we wish to form a preliminary estimate of the reliability of specifying high winds over the Middle Atlantic Continental Shelf by these methods.

[1] Present affiliation: Pacific Marine Environmental Laboratory, Environmental Research Laboratories, NOAA, Seattle, Wash. 98105.

2. Data sources

The two NOAA buoys (EB34 and EB41) were placed in service in October 1975. EB34 is located southeast of New York City at 40.1°N, 73.0°W, and EB41 100 km off the New Jersey coast at 38.7°N, 73.6°W (Fig. 1). The buoys are both equipped with vortex shedding type anemometers at a height of 5 m. The averaging interval for speed and direction is 8.5 min. Both buoys also provide pressure, air temperature and water temperature measurements. EB41 is equipped with an accelerometer to estimate surface wave parameters. The buoys are interrogated by a shore collection station with the data entered into the Global Telecommunications System. Twelve percent of the hourly values for the 5 months of this study were missing.

Objective analyses of sea level pressure and surface air temperature on the Limited-Area Fine-Mesh (LFM) model grid currently in use at the National Meteorological Center (NMC) are completed twice daily at 0000 and 1200 GMT. The techniques used are essentially those reported on by Cressman (1959), although numerous modifications to his procedures have been adopted over the years. At 39°N the grid length is ~166 km, and since the grid is oriented along 105°W, it is almost parallel to the New Jersey coastline. There are normally 25 land stations and between 5 and 15 ship reports used in the analyses for the region bounded by Cape Hatteras to the south, Cape Cod to the north, one grid length landward and two grid lengths seaward of the coastline. The first guess fields are 12 h numerical forecasts. For general eastward flow these fore-

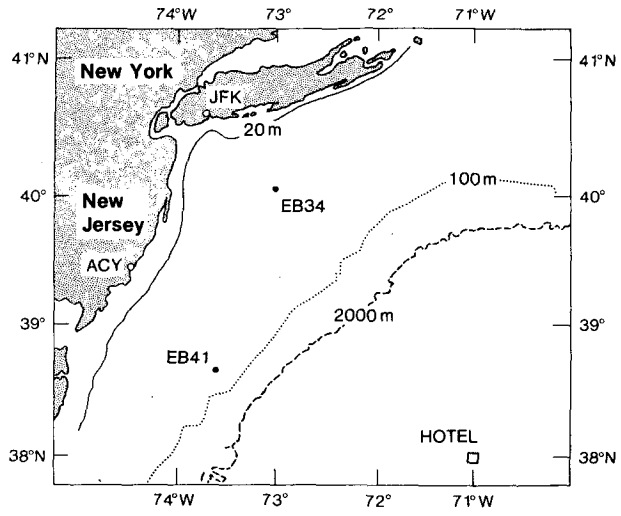

FIG. 1. Location map of the two NOAA buoys, EB34 and EB41.

casts are initialized over the data-rich eastern United States.

For this study geostrophic wind estimates are obtained by bi-quadratically interpolating the pressure field to a grid with one-fourth the LFM grid length, applying a short wavelength smoother (Shuman, 1957), and estimating pressure gradients by central differences on the fine grid. Gradient winds are numerically estimated from isobar curvature (Endlich, 1961) on the fine grid and for anticyclonic curvature are limited to 130% of the geostrophic wind speed. Wind components are then interpolated to the buoy locations. For the months of November–January, the rms difference of the geostrophic wind component computed directly from the measured pressures at EB34 and EB41 and the geostrophic wind component recomputed from the LFM pressure analysis for the same location is 3.2 m s^{-1}. This represents the magnitude of the baseline error introduced by the interpolation and smoothing of the analysis scheme.

3. Summary of weather conditions for the winter of 1975–76

The winter of 1975–76 was noted for its extremely mild temperatures over much of the eastern United States. The 700 mb flow pattern was characterized by a large northward displacement of the jet from its normal winter position. The westerlies in the subtropics were weaker than normal, which was reflected in a winter devoid of storm development in the Gulf of Mexico. North of 35°N, storm tracks were primarily continental in origin, passing to the north of the buoy locations. One exception to this rather quiet winter was the storm of 1–3 February 1976, which intensified rapidly as it moved northeasterly along the east coast of the United States.

TABLE 1. Percent of wind observations by categories. Total of 3212 observations November 1975–March 1976 at EB34.

Wind speed (m s^{-1})	Direction NE	E	SE	S	SW	W	NW	N	Total
0–5	3.1	2.0	1.7	2.6	2.7	3.1	3.5	2.5	21.2
5–10	6.7	3.1	3.3	2.5	7.2	12.2	6.5	9.0	50.5
10–15	2.5	1.8	1.5	0.4	2.9	4.7	3.3	9.1	26.2
15–20	0.3	0.3	0.0	0.0	0.0	0.1	0.4	1.0	2.1
Total	12.6	7.2	6.5	5.5	12.8	20.1	13.7	21.6	100.0

TABLE 2. Percent of observations by wind speed and air-sea temperature difference classes. Total of 3177 observations November 1975–March 1976 at EB34.

Wind speed (m s^{-1})	Air-sea temperature difference (°C) <−10	−10 to −6	−6 to −2	−2 to 2	2 to 6	Total
0–5	1.8	3.9	4.7	10.1	0.8	21.3
5–10	2.2	6.0	13.4	23.6	5.3	50.5
10–15	3.0	5.4	6.7	6.3	4.7	26.1
15–20	0.3	0.9	0.5	0.3	0.1	2.1
Total	7.3	16.2	25.3	40.3	10.9	100.0

a. *Wind observations*

Percentages of hourly observations of wind speed and direction for the 5-month period by classes are given in Table 1, based upon data from EB34. Wind speeds in excess of 10 m s^{-1}, predominantly from the north, account for 28.3% of the observations during the 5-month period.

b. *Air and sea temperature*

During the late fall and early winter, strong continental influence resulted in large fluctuations of air temperature recorded at the buoys. Cold air masses surged out over the shelf region, dropping air temperature rapidly; then the temperature would moderate from the influence of the ocean environment before the next cold surge. The distribution of air-sea temperature differences for the 5-month period is summarized in Table 2.

4. Model description

This section reviews methods for estimating surface winds and the next section discusses results.

a. *Model 1 (Cardone)*

The first approach is to estimate anemometer height winds from the LFM pressure analysis by means of a baroclinic, stability-dependent, marine boundary layer model proposed by Cardone (1969). A brief review of Cardone's model is provided in the Appendix. We take Cardone's model to be representative of the class of

analytical single point models. It has dependencies of the geostrophic drag coefficient and inflow angle on stability and thermal wind roughly comparable to similarity approaches such as Arya and Wyngaard (1975). Input data are the gradient wind and surface temperature field as specified from the LFM analyses and the sea surface temperature at the buoy locations.

b. *Model 2 (empirical)*

To contrast with Model 1, we have developed linear relations between buoy wind speed S and gradient wind speed G based upon the 5 months of data at EB34 and EB41. As there are observational errors in both parameters, particularly the gradient wind, we have adopted the Maximum Likelihood (ML) approach (Kendall and Stuart, 1967, p. 379), which computes the linear best fit constants of $S = \alpha_0 + \alpha_1 G$ as

$$\alpha_0 = \bar{S} - \alpha_1 \bar{G}, \tag{1}$$

$$\alpha_1 = \frac{\sigma_S^2 - \xi_S^2}{\sigma_{SG}^2}, \tag{2}$$

where the bar denotes sample mean, σ_S^2 is the sample variance of S, ξ_S^2 the observational error variance of S, and σ_{SG}^2 the sample covariance between S and G. Withee (1976) reports a total system accuracy standard deviation for wind speed measurements on EB34–EB41 type buoys of 0.3 m s^{-1} under moderate and severe environmental conditions. Fig. 2 plots the ML line of best fit for a composite of data from both buoys (solid line) and for each buoy separately (broken lines). The data set consists of observed surface winds >7.5 m s^{-1}. Instead of plotting all paired gradient and buoy speeds, the composite data set was ordered by increasing buoy wind speed into groups of 15 observations. Each dot on Fig. 2 represents the average value of buoy wind speed and gradient wind speed for each group. Slopes computed from (2) are nearly equivalent to a linear regression of G on S. Equations for the ML best-fit lines are given in Table 3 in addition to the mean inflow angle for unstable ($\Delta T < -2.0$) and neutral-stable ($\Delta T > -2.0$) classes. Model 2 will specify the line of best fit for wind speed and the mean inflow angle for the two stability classes as developed from the composite data set.

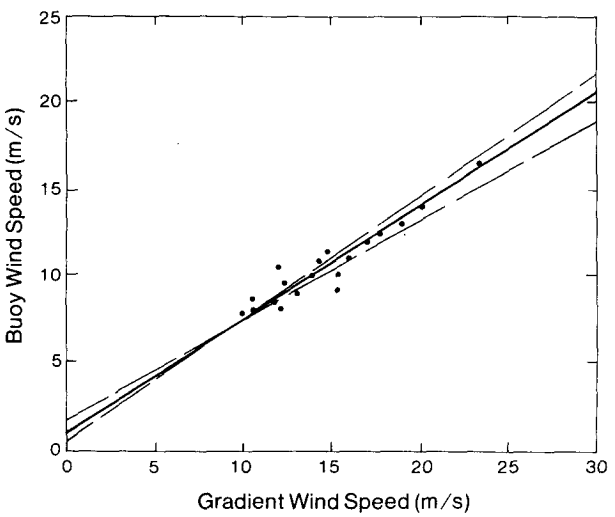

FIG. 2. Plot of maximum likelihood best fit of buoy wind speed and gradient wind speed estimated from the LFM pressure analyses. The dashed lines represent the best fit for each buoy and the solid line is the best fit for a composite of data from both buoys.

TABLE 3. Equations for ML best fit of buoy wind speed S and gradient wind speed G and inflow angle, for unstable ($\Delta T < -2.0$°C) and neutral-stable ($\Delta T > -2.0$°C) classes. Data set consists of buoy observations with wind speed >7.5 m s^{-1}.

Data set	Composite	EB34	EB41
Number of observations			
Total	290	150	140
Unstable	153	78	75
Neutral-stable	137	72	65
ML line of best fit (m s^{-1})	$S=1.0+0.65G$	$S=1.7+0.58G$	$S=0.5+0.71G$
Correlation	0.60	0.62	0.59
Mean inflow angle and standard deviation (deg)			
Unstable	24.0±21.5	20.7±26.0	27.4±15.1
Stable	30.7±26.6	27.2±25.1	34.7±28.0

c. *Model 3 (sea extrapolation)*

Model 3 represents direct application of EB41 wind velocity to the location of EB34, a distance of 165 km.

d. *Model 4 (land extrapolation)*

It had been planned to compare EB34 wind with those measured at JFK airport and EB41 winds with Atlantic City. However, of a total of 222 0000 and 1200 GMT observations with EB41 wind speeds >5 m s^{-1}, Atlantic City reported calm on 18 occasions. Ten of those 18 had buoy winds >7.5 m s^{-1}. It is concluded that coastal winds based upon Atlantic City are not reliable because of its inland location of 36 km. Model 4, as applied at EB34, will assume the same wind direction as JFK and increase the speed according to the line of best fit (ML method) under the assumption that the error variances

TABLE 4. Equation of ML best fit for estimating wind speed at EB34 from wind speed at the JFK Airport Weather Service Forecast Office. Based upon 3 h data with 0000 and 1200 GMT excluded.

Number of observations	Equation of ML best fit (m s^{-1})	Correlation
792	$U_{EB34}=0.5+1.41U_{JFK}$	0.66

TABLE 5. Geostrophic, gradient, observed and model-estimated wind speed (m s^{-1}) and inflow angle (deg) for buoy observed wind speeds >15.0 m s^{-1}.

Month Day Hour	Air-sea temperature (°C)	Geostrophic speed (m s^{-1})	Gradient speed (m s^{-1})	Observed Speed	Observed Inflow	Model 1 Speed	Model 1 Inflow	Model 2 Speed	Model 2 Inflow	Model 3 Speed	Model 3 Inflow	Model 4 Speed	Model 4 Inflow
EB34 data													
12 22 1200	−9.0	32.6	25.5	15.9	23.0	14.6	36.0	17.6	24.0	15.0	32.0	14.8	31.0
12 23 0000	−10.0	30.8	26.4	15.7	27.0	16.4	31.0	18.1	24.0	17.5	44.0	11.1	43.0
01 04 1200	−8.2	17.7	21.3	15.4	44.0	14.9	27.0	14.8	24.0	11.7	17.0	18.4	37.0
01 14 1200	−0.2	27.0	24.0	15.5	29.0	13.8	24.0	16.6	31.0	17.6	19.0	14.8	22.0
01 22 1200	−8.4	27.2	22.2	16.3	30.0	15.0	25.0	15.4	24.0	15.8	34.0	14.8	25.0
01 23 0000	−12.5	19.3	20.6	16.3	33.0	17.5	29.0	14.4	24.0	15.9	44.0	19.8	36.0
03 17 1200	−7.0	26.5	23.3	16.0	19.0	16.5	22.0	16.1	24.0	15.9	25.0	19.8	18.0
Mean	−7.9	25.9	23.3	15.9	29.0	15.5	28.0	16.2	25.0	15.6	31.0	16.6	30.0
EB41 data													
11 24 1200	−2.9	44.0	31.6	15.7	48.0	14.0	21.0	21.5	24.0				
12 22 1200	−9.8	24.9	19.3	15.0	16.0	12.4	33.0	13.6	24.0				
12 23 0000	−10.3	26.5	20.1	17.5	31.0	13.8	29.0	14.0	24.0				
01 14 1200	−0.5	20.6	20.0	17.6	19.0	12.8	25.0	14.0	31.0				
01 22 1200	−8.6	23.2	20.4	15.8	26.0	14.0	22.0	14.3	24.0				
01 23 0000	−8.6	15.4	19.0	15.9	57.0	14.8	31.0	13.4	24.0				
02 02 1200	−7.4	48.6	33.1	22.5	40.0	23.2	32.0	22.5	24.0				
03 17 1200	−5.1	23.1	22.6	15.9	24.0	15.3	21.0	15.7	24.0				
Mean	−6.7	28.3	23.3	17.0	33.0	15.0	27.0	16.1	25.0				

of both anemometers are equivalent (Table 4). Table 4 is based upon paired data at 3 h intervals for the 5-month period with 0000 and 1200 GMT data excluded.

5. Application

a. *Gradient wind*

Table 5 lists the LFM geostrophic, gradient, observed and model-estimated surface winds for both EB34 and EB41 for those cases with observed winds >15.0 m s^{-1}. In almost all cases, making gradient corrections to the geostrophic wind provides better agreement between observed and model-estimated surface winds than would basing the model winds on geostrophic winds. Using EB34, for example, at 0000 GMT 23 December 1975, the geostrophic wind is 30.8 m s^{-1}, the gradient wind is 26.4 m s^{-1}, Cardone's model gives 16.4 m s^{-1} (based on gradient wind), and the observed surface wind is 15.7 m s^{-1}.

b. *Model comparison*

Table 6 lists the mean magnitude of the vector error (hereafter referred to as the mean absolute error), rms vector error, and mean and standard deviation of speed and direction error by speed classes obtained by verifying model estimates against EB34. Three of the

TABLE 6. Comparison of error statistics for the four methods of specifying winds. Verification is against 0000 and 1200 GMT data at EB34.

Model	Speed class (m s^{-1})	Count	Mean absolute error (m s^{-1})	Rms vector error (m s^{-1})	Mean speed error (m s^{-1})	Speed standard deviation (m s^{-1})	Mean inflow error (deg)	Inflow standard deviation (deg)
Model 1 (Cardone)	$S<5$	59	2.92	3.58	−1.07	2.37	−17.5	43.9
	$5\leqslant S<12.5$	191	3.49	3.98	0.98	2.37	−7.8	26.0
	$12.5\leqslant S$	22	2.93	3.35	0.39	2.40	−1.2	10.2
Model 2 (Empirical)	$S<5$	59	3.31	3.88	−2.04	2.29	−0.5	41.7
	$5\leqslant S<12.5$	191	3.44	4.14	−0.40	2.94	2.4	24.8
	$12.5\leqslant S$	22	3.29	3.71	−1.13	2.62	0.7	10.0
Model 3 (Extrapolate from EB41)	$S<5$	56	2.86	3.17	−1.16	1.90	13.0	51.9
	$5\leqslant S<12.5$	185	3.14	3.84	0.44	2.11	9.6	28.2
	$12.5\leqslant S$	22	3.31	4.21	0.46	1.64	8.9	16.0
Model 4 (Extrapolate from JFK)	$S<5$	59	4.07	4.66	−1.35	2.65	6.0	76.5
	$5\leqslant S<12.5$	191	3.79	4.59	0.62	2.63	3.6	32.4
	$12.5\leqslant S$	22	3.88	4.46	1.32	2.68	5.9	15.3

methods have roughly comparable error levels, with Model 4 (extrapolation from JFK) somewhat poorer.

Cardone's model effectively tunes to the regional climatology by inclusion of air stability and thermal wind. For example, neglect of the strong baroclinicity associated with the temperature gradient established between cold continental air and the Gulf Stream region increases the mean absolute error of Cardone's model from 2.9 to 3.8 m s^{-1} at high wind speeds. The largest errors in both Cardone's and the empirical model were caused by the same errors in estimates of the geostrophic wind, particularly in the vicinity of fronts. We conclude that Cardone's model is comparable to seasonally and regionally dependent empirical values when both are based upon routine synoptic pressure analyses.

Errors in the extrapolation-based models occurred primarily when station distances were a significant fraction of storm size, resulting in larger standard deviations of inflow angle than with pressure-gradient-based models.

c. *Temporal variability*

Fig. 3 plots the mean and mean absolute value of observation-to-observation variability of wind direction and speed for lagged, paired observations at EB34. Considering that these values are 5-month means, average direction changes of 33° and speed changes of 2.3 m s^{-1} in 6 h are indicative of rapidly moving and probably developing storm systems. Titov (1969, p. 112) indicates that for wave forecasting it is necessary to resolve relative changes of 2 m s^{-1} in speed and 25° in direction. If we adopt this working definition for wind-driven currents, then Fig. 3 suggests that pressure analyses are necessary on a minimum of a 6 h cycle to confidently interpolate between analyses.

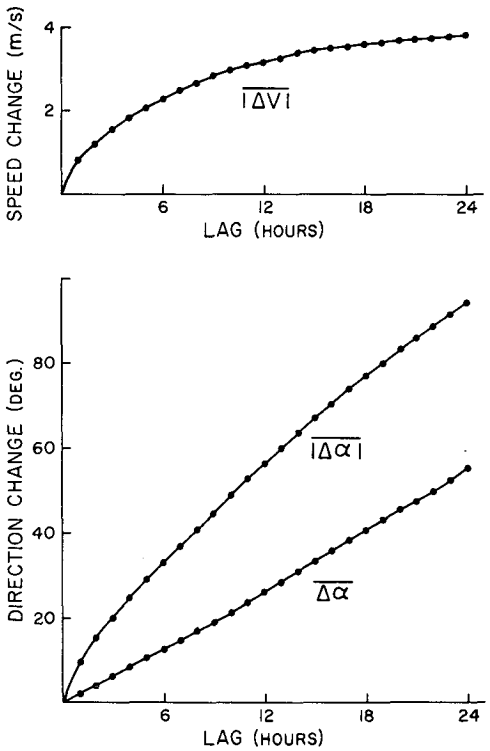

FIG. 3. Observation-to-observation variability in wind velocity at EB34. The average change in direction ($\overline{\Delta\alpha}$) and the average absolute value of the change in direction ($\overline{|\Delta\alpha|}$) and speed ($\overline{|\Delta v|}$) are plotted as a function of separation interval.

6. Conclusions

We have investigated the two simplest methods of specifying winds: extrapolation and inference from pressure analyses. The study was predicted on the existence of 5-month time series from two coastal buoys and considers a single winter season.

Extrapolation from nearby buoys depends on the ratio of the separation distance to storm size. Reliability is based upon the adequacy of the sensor and communication system. Of 304 possible 0000 or 1200 GMT observations, EB34 failed on 24 occasions and EB41 on 21.

Extrapolation from land by simple methods was determined to be the least reliable approach. Agreement should improve by lagging the estimates in time and averaging over several coastal stations; however, basic land-water contrasts remain. Summer sea breeze circulation and local orographic features such as those reported by Halpern (1976) would further aggravate the situation, as would urban-induced effects (Bornstein and Johnson, 1977).

Surface winds estimated from synoptic fields show a larger error from estimating input parameters such as the geostrophic wind than from choosing one boundary layer model over another. Analysis schemes which incorporate multiparameter boundary layer models should take into account the range of expected errors of the input parameters. For winds in excess of 10 m s^{-1}, the LFM-based analyses provided adequate specification of the offshore wind field 81% of the time, defined by having a mean absolute error <5 m s^{-1}. The remaining 19% included underestimation of detail structure in the vicinity of fronts.

Acknowledgments. We wish to thank V. Cardone for making available copies of his computer programs. We appreciate the assistance provided by A. Johnson and his associates of the NOAA Data Buoy Office and by A. Nierow and S. Rich of the National Meteorological Center.

APPENDIX

Computational Formulas

Cardone's model separates the boundary layer into two regions, a surface layer and an Ekman layer.

The wind in the surface layer is specified by

$$U=\frac{U_*}{K}\left[\ln\left(\frac{Z}{Z_0}\right)-\Psi\left(\frac{Z}{L'}\right)\right], \tag{A1}$$

in which U is the wind speed, $U_*=(\tau/\rho)^{\frac{1}{2}}$, τ is the surface stress, ρ is the air density, $K=0.4$, Z is height, Z_0 is the roughness parameter and L' is a modified form of the Monin-Obukov stability length, i.e.,

$$L'=\frac{U_*^2\bar{\theta}[\ln(Z_a/Z_0)-\Psi(Z_a/L')]}{K^2g(\theta_a-\theta_s)}, \tag{A2}$$

in which g is the acceleration of gravity and θ is temperature. Anemometer level parameters are identified by the subscript a and θ_s is the sea surface temperature. The stability dependence function Ψ is defined as

$$\Psi(Z/L')=\int_{Z_0/L'}^{Z/L'}\frac{[1-\Phi(\xi)]}{\xi}d\xi, \tag{A3}$$

where $\Phi(Z/L')$ is given as

$$\text{STABLE}\quad \Phi=1+B'(Z/L')/(1+Z/L') \tag{A3a}$$

$$\text{UNSTABLE}\quad \Phi^4-(\delta'Z/L')\Phi^3-1=0 \tag{A3b}$$

with $B'=7$ and $\delta'=18$. Eq. (A3a) is our modification of Cardone's original log-linear profile to extend its range of applicability to larger air-sea temperature differences (Kondo, 1975). Wave development is considered indirectly through the dependence of surface roughness Z_0(cm) upon U_* given by

$$Z_0=(0.684/U_*)+4.28\times10^{-5}U_*^2-4.43\times10^{-2}. \tag{A4}$$

The upper layer is an Ekman solution with a constant eddy viscosity K_M. The height h of the surface layer is specified explicitly in terms of external parameters, i.e.,

$$h=B_0G/f, \tag{A5}$$

where G is the wind speed at the top of the Ekman layer, f the Coriolis parameter and B_0 an assignable constant taken from Blackadar (1965) to be 3.0×10^{-4}. The eddy viscosity in the upper layer is specified by

$$K_M=KU_*h/\Phi(h/L'). \tag{A6}$$

The solution for inflow angle β and geostrophic drag coefficient is determined from the equations for each layer by imposing conditions of continuity of wind and wind shear at the interface. For the barotropic case, these are

$$\frac{U_*}{G}=[2KB_0\sin^2\beta/\Phi(h/L')]^{\frac{1}{2}}, \tag{A7}$$

$$\frac{U_*}{G}=\frac{\sqrt{2}K\sin\left(\frac{\pi}{4}-\beta\right)}{\ln\frac{B_0G}{fZ_0}-\Psi(h/L')}, \tag{A8}$$

and along with (A2) and (A4) form a closed system that can be solved by iteration. For the baroclinic case, Eqs. (A7) and (A8) are modified by the introduction of geostrophic shear through a nondimensional thermal wind parameter

$$T_w=\frac{1}{f}\left|\frac{\partial G}{\partial Z}\right|,$$

and the angle between the thermal wind and the surface geostrophic wind. These modified equations are given both by Cardone (1969) and Isozaki and Uji (1974).

REFERENCES

Arya, S. P. S., and J. C. Wyngaard, 1975: Effect of baroclinicity on wind profiles and the geostrophic drag law for the convective planetary boundary layer. *J. Atmos. Sci.*, **32**, 767–778.

Beardsley, R. C., and B. Butman, 1974: Circulation on the New England Shelf: Response to strong winter storms. *Geophys. Res. Lett.*, **1**, 181–184.

Blackadar, A. K., 1965: A simplified two-layer model of the baroclinic neutral atmospheric boundary layer. Air Force Cambridge Res. Lab. Rep. 65–531, 49–65.

Bornstein, R., and D. Johnson, 1977: Urban-rural wind velocity differences. *Atmos. Environ.* (in press).

Cardone, V. J., 1969: Specification of the wind distribution in the marine boundary layer for wave forecasting. Rep. GSL-TR69-1, New York University, School of Engineering and Sciences, 131 pp.

Cressman, G., 1959: An operational objective analysis system. *Mon. Wea. Rev.*, **87**, 367–374.

Endlich, R. M., 1961: Computation and uses of gradient winds. *Mon. Wea. Rev.*, **89**, 187–191.

Halpern, D., 1976: Measurements of near-surface wind stress over an upwelling region near the Oregon coast. *J. Phys. Oceanogr.*, **6**, 108–112.

Isozaki, I., and T. Uji, 1974: Numerical model of marine surface winds and its application to the prediction of ocean wind waves. *Pap. Meteor. Geophys.*, **25**, 197–231.

Kendall, M. G., and A. Stuart, 1967: *The Advanced Theory of Statistics*, Vol. 2, *Inference and Relationship*. Charles Griffin & Co., Ltd., 690 pp.

Kondo, J., 1975: Air-sea bulk transfer coefficients in diabatic conditions. *Bound.-Layer Meteor.*, **9**, 91–112.

Schuman, F. G., 1957: Numerical methods in weather prediction: II. Smoothing and filtering. *Mon. Wea. Rev.*, **85**, 357–361.

Titov, L. F., 1969: *Wind-Driven Waves*. Gidrometeor. Leningrad, 243 pp. [English translation available from NTIS.]

Withee, G. W., 1976: Data quality statement for NOAA Data Buoy Office Moored Data Buoys, Data Quality Division. NOAA Data Buoy Office, Bay St. Louis, Miss., 76 pp.